Team SNU MACRO
RobotX Journal Paper

Jooho Lee, Joohyun Woo, Hwiyong Choi, Woohyun Jung, Hujae Choi, Nakwan Kim

Abstract— **This paper describes about Team SNU MACRO's Autonomous Surface Vehicle (ASV) system that is developed for 2016 Maritime RobotX Challenge. After outlining our system's major hardware and software components, we focus on describing our strategy to complete eight competition tasks. Based on a bare-platform WAM-V, our team developed propulsion, laucher and electronic system. Propulsion system was designed to obtain basic surge, sway and yaw motion and additional motion like dynamic positioning and point of interest motion to help complete some tasks. For detecting and interpreting objects on surface and even underwater, lidar, cameras and hydrophone composed perception system. Racquetball laucher system was developed for carrying out newly added task 'detect and deliver' inspired by pneumatic tennis ball launcher. Mission planning is carried out by hierarchical state machine that generates to perform the tasks considering exception. Software was developed for each mission in Labview environment and integrated after all codes were tested in simulations. Field experiments was conducted to validate each hardware and software systems and to check the performance and robustness of our integrated system.**

I. INTRODUCTION

In recents years, lots of attention and attepts have been made to intelligent and autonomous vehicle system. In maritime domain, ASV also have been developed for marine science, bathymetric mapping and military operation [1]. Performing a hazardous, tedious and tough operation without human worker or operatator, it makes ASV irreplaceable.

The 2nd Maritime RobotX Challenge is the international competition organized by the Association for Unmanned Vehicle Systems International (AUVSI) Foundation and NAVATEK and sponsored by the U.S Office of the Naval Research (ONR) with the goal of creating a new, high-level competition about ASV. The specific goal of this competition is to complete certain tasks without human intervention. Those tasks are including: 1) demonstrate navigation and control, 2) find totems and avoid obstacles, 3) identify symbols and dock, 4) scan the code, 5) underwater shape identification, 6) find the break, 7) detect and deliver, and 8) acoustic pinger-based transit.

Using a bare-platform WAM-V which was provide by last competition, we focused on designing and developing the propulsion, launcher and electronic system suitable to given platform and those tasks. Software system was developed in Labview environment to perceive nearby environment using onboard senser and to operate the actuators which can generate desired motion.

Through several field tests which was built similar to competition area, we validated developed hardware system and individual task's capability.

The rest of this paper is organized as follows. In section 2, the system architecture of our ASV system is described. And our approaches to perform the competition tasks are described in section 3. Finally, section 4 is described the conclusion of this study.

Fig. 1. MACS: the SNU MACRO team vehicle

II. SYSTEM DEVELOPMENT

A. Computer System

Our computer systems are consist of two computer. First one is mapping computer, which can deal with processing of LIDAR data and camera informations. This computer deals with perception process of ASV, and most of the perception related decision is made by this computer. ADlink MXE-5501 industrial PC is used for the mapping computer. It has 6th Gen Intel Core i7 Processor and 8G DDR4 RAM on it.

Another computer deals with lower level hierarchy issues. National Instrument compact RIO 9024 computer is used as control computer. It collect navigation related sensors (GPS, GPS compass, AHRS) data to generate navigational solution. In addition, once control command is calculated, it generate analog signal to deliver it to motor control unit.

Both of our compters are industrial PC which can deal with hazardous conditions ASV might face, such as vibration, impact, temperature, humidity and so on.

B. Perception System

The ASV is equipped with a 2D Lidar(SICK LMS511) and two monocular cameras(Pointgrey Blackfly and SJ 4000) to detect and identify various objects, symbols, or structures

on water surface. They are mounted at the front of the deck. 2D Lidar has FOV of 190° and its maximum detection range is 80 meters. A nodding system that tilts the Lidar up and down is applied to eliminate blind spots of 2D lidar. The maximum nodding period is upto 2Hz. Two cameras are installed under the Lidar and its nodding system. One has FOV of 110° and the frame rate is 30 fps. The other has FOV of 130° and the frame rate is 30 fps. Lidar and monocular cameras are co-calibrated and this information is used to calculate image ROI using LIDAR measurement in *Scan the code*, *Identify symbols and dock* and *Detect and Deliver.*

Besides these two main camera, two additional analog cameras are equipped for the particular tasks, *underwater shape identification* and *detect and deliver.* one of these cameras is mounted under the surface near hydrophone for the underwater shape identification, and the other one is installed at the front of the racquetball launcher for visual servoing of the launcher module. Camera control module switches the analog signals of two cameras using relay in order to get the right image signal for a particular mission.

C. Hydrophone System

Two Hydrophones (Redone Technologies) are installed at the stern side of the WAM-V. One is installed at the port side and another is installed at the starboard side. They are submerged approximately 0.6 m in depth.

The Hydrophones are connected to a preprocessor (4ch. Acoustic module v1.0, Redone Technologies) which performs filtering, amplifying and ADC. An embedded board (Beaglebone Black, Texas Instrument) are installed to calculate DoA (Direction of Arrival) from the pinger signal. Embedded board receives acoustic signal samples over TCP/IP socket communication from the preprocessor. After the calculate of DoA, the board sends the DoA to the mapping PC over the USB cable using TCP/IP socket communication.

Fig. 2. Hydrophone and preprocessor used for acoustic sound detection

D. Racquetball Launcher System

Among various ways to deliver racquetball, our team chose to use pneumatic based racquet ball launch system. Our pneumatic racquet ball launch system consists of two modules. First one is compression module. It consists of compressor (12V-150W), reservoir, and solenoid valve (12V). When aiming is ready, the solenoid valve is open and compressed air is suddenly released through the air hose and propel the racquet ball. Reservoir was made of PVC pipe (VG1), which can allow pressure upto 340psi. We launch the ball at about 70 psi, and it is fast enough to generate straight

linear motion toward to the target hole.

Launching module is consists of 3 motors (two for aiming, one for reloading), gunbarrel, revolver for reloading, and camera. ROBOTIS MX-64 and MX-106 motors are used to control launching module. Gun barrel and revolver parts are specially designed for this task and produced by using 3D printer. On the top of the gun barrel, aiming camera is located so that we can use visual servoing technique for aiming.

After the ball is launched, reloading precess is immediately followed. the gunbarrel will tilt up, then the revolver rotates to put the next ball in barrel, after that, the gunbarrel will tilt down to its initial position. While reloading is in progress, the compression process also proceeds at the same time. it needs 10 seconds to compress the air up to 70 psi.
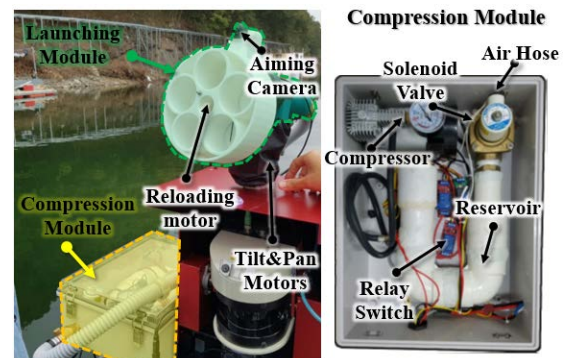
Fig. 3. Pneumatic racquet ball launcher system

E. Propulsion-System

The propulsion system consists of main thruster system and side thruster system. There are two main thrusters mounted on stern side of each of the pontoons. Two Minnkota RT160EM motors are used as main thrusters, and it can generate speed approximately up to 4 knots. Besides of main thrusters, at this time we have decided to use side thrust system as well. Two Minnkota Endura 55 pounds motors are mounted at each side of the pontoons. One of the characteristics of our side thruster system is that its installation location. Side thrusters are often installed at the bow side of ship (so called "bow thruster"). Instead of this, we decided to install side thruster as close as possible to longitudinal center of gravity, in order to decouple yaw motion and sway motion as much as possible. By doing so, we can decouple each motion as independent mode, and controller design become much simple and we don't need to consider about thrust allocation problem.
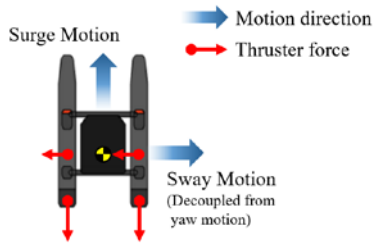
Fig. 4. Layout of the main and side thruster systems

F. Guidance-Navitaion-Control System

Guidance – Navigation – Control (GNC) systems are one of the most crutial parts of an autonomous system. For navigation, we adopted kalman filter based navigation filter which can combine global positioning system(GPS) and inertial measurement unit (IMU) data. We used loosely coupled integration technique for calculating high precision ASV navigation solution.

For guidance and control, we defined several motion mode in order to deal with some of the task requirement. For example, in *detect and deliver* task, ASV should find designated side of the tower. Since our monocular camera is mounted at front side of ASV, it would be beneficial to revolve the tower while ASV is always looking at the tower. As a result of this, we have developed point of interest(POI) maneuver motion mode using side thruster system.(Fig 5) In this mode, desired heading angle is defined as line of sight(LOS) angle toward the point, while surge speed and radius of the turning is tuned by the operator. We also have developed path tracking mode for tracking of a path, pure sway mode *for identify symbols and dock* task, dynamic positioning mode for pose stabilization for LIDAR mapping.
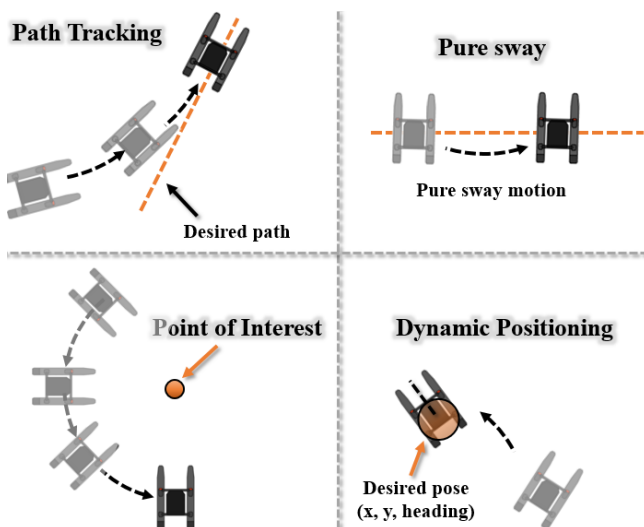
Fig. 5. Several motion mode developed to deal with some of the task requirements

III. TASK STRATEGIES AND ALGORITHMS

During the preparation process we have developed and improved strategies and algorithms for each of the eight tasks. Following sections are some of the brief description about the strategies and algorithms.

A. Find Totems and Avoid Obstacle

Find totmes and avoid obstacle task has the largest mission area among 8 missions. When ASV is initially planning its action, ASV can not aware of every information of obstacles and totems due to lack of observability. Which means, in order to go through this task, it is not sufficient to use offline method. As ASV proceed missions, new information will be perceived, and by using the renewed information, motion planning should be performed simultaneously. In order to successfully solve this task, we have divided task state into mainly 3 parts.

First state is called *Goal position tracking*. In this state, LIDAR measures relative position between ASV and ostacles. Once obstacle's position can be calculated, these information is tracked by using Kalman filter. After that, based on the tracked information, a Gridmap can be calculated. In this *Goal position tracking* state, A* search algorithm[2] is used to generate safe path to the goal position. Fig 6 (left) shows Kalman filter tracking result of obstacle information. Radius of the each obstacle represents uncertainty level of obstacle. Fig 6 (right) represents grid map of the corresponding obstacle tracking result and planned safe path. As obstacle map is updated, due to measurement error or uncertainty of the environment, planned path can be considered as dangerous. In this case, based on the renewed obstacle map, path planning algorithm will regenerate safe path to track.
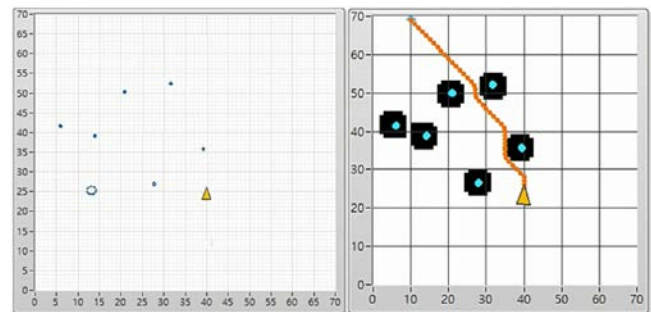
Fig. 6. Obstacle tracking result(left) and path planning result (right)

In the *Goal position tracking* state, ASV changes goal position consistently as it proceed the task. At the beginning, it initially tracks final point of the mission coordinate. However, once any colored buoy is detected on search domain in camera image (Fig 7), and its Kalman filter tracking result (uncertainty level) satisfies certain level, the goal position changes to direction of the detected obstacle.

After that, while ASV is tracking the colored obstacle, if the colored object reaches to turning domain (Fig 7) of the camera image, the state changes to *turning maneuver* state. At the turning maneuver state, ASV performs POI maneuver with designated direction of the color. Although ASV is tracking safe avoidance path generated from A* search algorithm, due to imperfection of mapping process or path

tracking error, ASV may enter dangerous region, where close to obstacle buoy. In this case, *reflexive avoidance*[3] state can be activated. *Reflexive avoidance* is low-level avoidance maneuver where it generates pure sway motion to avoid detected target. After certain time passes, it changes back to *Goal position tracking* state.

Fig. 6. Camera Image during Find Totems and Avoid Obstacle Task

B. Identify symbols and Dock

In the identify symbols and dock task, the ASV autonomously enters to the two designated bays sequentially. The ASV perform the task in three steps. At first, it locates each docking bays using Lidar scanning data and dock's geometrical information. After the detection of the dock, it identifies each symbol of bays using Lidar and camera. Desired path from current position and the entrance of objective bay is generated based on symbol identification result and predefined location of bays. Before proceeding into the bay, lateral position alignment is conducted to minimize a collision risk.

In order to specify the location of docking bays and symbols, line segments which are composed of three blobs are detected from the clustered LIDAR data. Among the detected line segments, a line which has the most similarities with predefined geometrical information of the dock is extracted. Finally, the location of bays and symbols in mission coordinate is defined based on the extracted line.

Experiment results of dock and symbols detection is represented in Fig 7. In Fig 7, top figure shows top view of task area in Jangseong-lake where the docking experiment is conducted and two figures in the right side show the detection results. There are two docking bays available to perform docking in Jangseong-lake. For this reason, it is assumed that bay 2 and 3 have same location and direction.
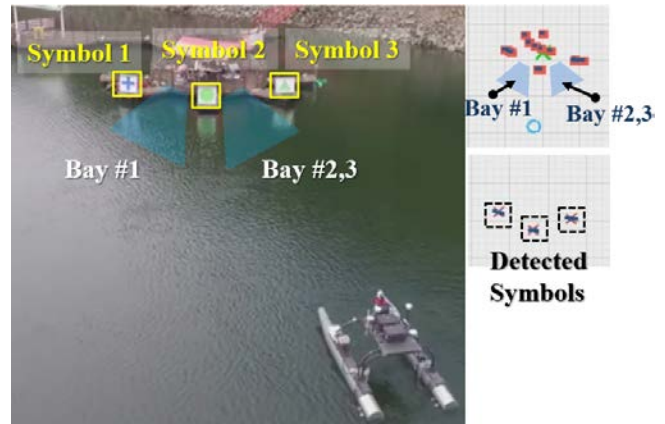
Fig. 7. Top view of the identify symbols and dock task area. Dock and symbols detection results(right).

After locating symbols, the ROIs of three symbols in image pixel frame for the symbol identification is defined by using LIDAR-camera calibration information and LIDAR scanning data. Template matching[4] is used to identify the shape using the binary image created by color and intensity thresholding process. The color is classified by comparing Euclidean distance between average hue and saturation value in ROI and its predefined thresholding values of each color. Based on the accumulated results for a certain period of time, the final identification result for each symbols are obtained by voting. Desired path from the current position of the ASV to the first and second objective bay is generated using previously obtained locations of each bay and the results of symbols identification. Fig 8 shows the binary image created by image processing and symbol identification results when the symbols from left to right are blue cruciform, green circle, and green triangle.
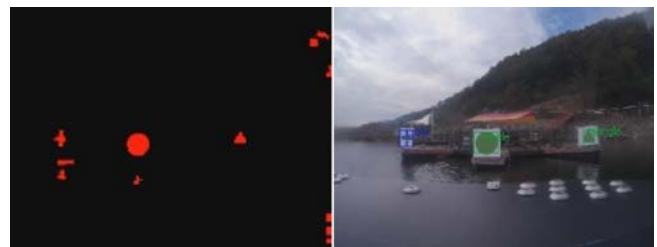
Fig. 8. Binary image from image processing and symbols identification results

When the ASV enters to the bay, there exists a risk of collision due to the uncertainty of locations of bays which are based on Lidar scanning data measured from a distance. In addition, water flow disturbance running in lateral direction to the ASV could interfere with entry. In this reason, lateral position alignment is required to safe docking before proceeding into the bay.

After reaching the entrance of the objective bay, the ASV maps the left side of the bay using Lidar scanning. From the Lidar mapping data, the left prominent part of the bay is extracted. Lateral position alignment is carried out based on the relative distance between the ASV and the extracted

prominent part of the bay.
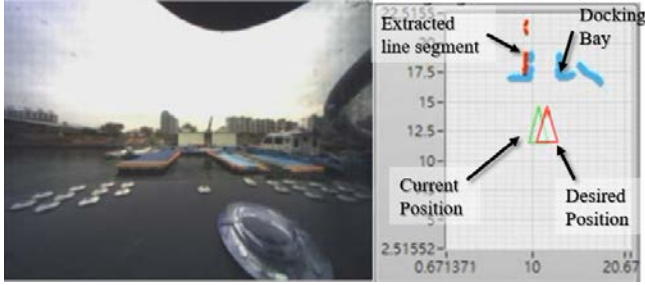
Fig. 9. Lateral position alignment stage of identify symbols and dock task

Snap shots of ASV carrying out docking task when the first objective symbol is blue and second one is triangle are in Fig 10.
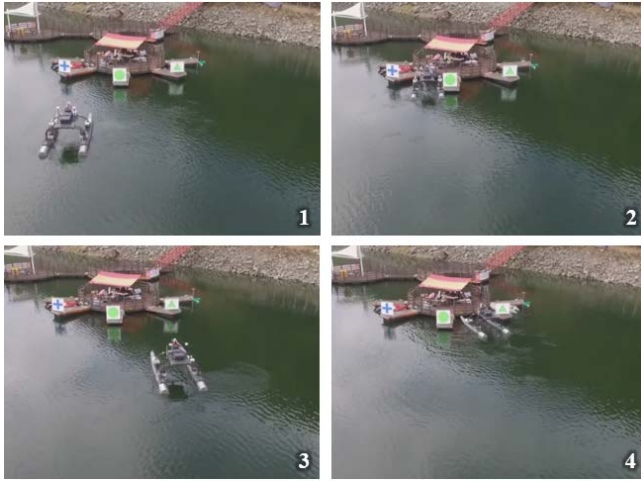
Fig. 10. Top views of ASV performing docking motions when the first objective symbol is blue and the second symbol is triangle.

C. Scan the Code

In this mission, the ASV is required to detect a randomly located light buoy in mission area and report the exact color sequence of buoy's light. Light buoy will display any three of the four colors: red, green, blue or yellow. Each displayed color will appear for 1 second, after LED will remain off for 2 seconds.

Before detecting and recognizing the LED region, the ASV must detect the ramdonly located light buoy using the lidar system. Once the light buoy is detected, the ASV approaches to the light bouy and performs a dynamic positioning maneuver in front of the light buoy. After that, a region of interest (ROI) which contains the LED bar can be calculated from by using LIDAR detection of the light tower. Using the relationship between co-calibrated camera and lidar, we can determine the position and size of the region of LED bar in the image plane. The recognition algorithm is divided into three step: preprocessing, extraction & tracking and recognition.

- **Preprocessing :** Vision based color detection in outdoor image is difficult problem mostly due to its varying lighting conditions. Especially, red-green-blue(RGB)

color model is known as the most sensitive model to the light condition change. So in preprocessing step, instead of RGB color model, we decided to use hue-saturation-value(HSV) color model which separates color component from intensity component.
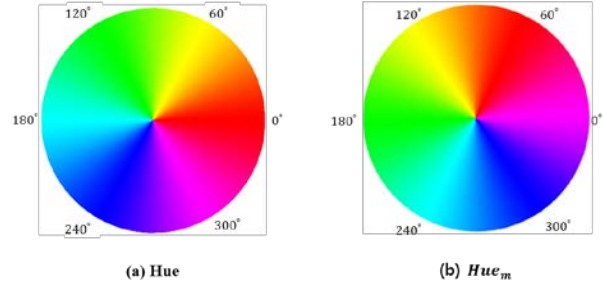
Fig. 11.Hue component of HSV color model

Red color in hue space is discontinous near 0 and 360 degree whereas hue component of yellow, green and blue is continous near 60, 120 and 240 degrees respectively, shown in Figure 2. So we do a mapping to build hue component of red color to be continuous. Let Hue_m be newly mapped hue variable:

$$Hue_m = \begin{cases} Hue + 60 & ; H \le 300 \\ Hue - 300 & ; H > 300 \end{cases}, \quad (1)$$

Then, hue component of red, yellow, green and blue is continuous near 60, 120, 180 and 300 degrees respectively.

- **Extraction & tracking:** The goal of this stage is extraction of the ROI (region of interest). When LED turns on. At that moment, saturation and intensity value in LED region suddenly increases. We can determine the LED region by analyzing consecutive two frames with sudden increasement of saturation and intensity threshold value. But after LED turns on, the extracted ROI must be updated because of ASV's drift motion. Once the ROI are extracted, we conduct the HSV histogram analysis. Then normal distribution of of hue, saturation and intensity in pixels in ROI can be obtained:

$$\begin{aligned} Hue_m &\sim N(\mu_{hue}, \alpha_{hue}) \\ Sat &\sim N(\mu_{sat}, \alpha_{sat}) \\ Val &\sim N(\mu_{val}, \alpha_{val}) \end{aligned}, \quad (2)$$

Assuming that if a pixel satisfies certain conditions, it belongs to ROI. So, we used color threshold method to do segmentation.

$$pixel_{ROI} \in \begin{cases} Hue_m \in [\mu_{hue} \pm a_{hue}] \\ Sat \in [\mu_{sat} \pm a_{sat}] \\ Val \in [\mu_{val} \pm a_{val}] \end{cases}, \quad (3)$$

By updating the ROI every frame, robust ROI tracking can be performed.

- **Recognition:** Using hue component's analysis result, we can make a decision of the current LED's color.

Calculating each Euclidean distance between current hue's mean value and four reference value, we determine the current LED color from shortest distance among four distance results.

(a) Red   **(b) Green**   **(c) Yellow**
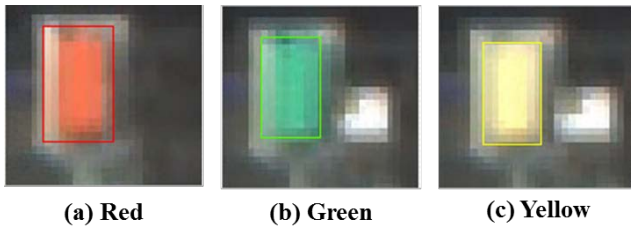
Fig. 12. Recognition results of the light buoy

Fig 12 shows the recognition results when the LED color was red, green and yellow respectively. The colored bounding box represents detected ROI and corresponding recognized color.

In order to determine and report final color pattern, ASV stores series of color sequence. After certain amount of time, using voting algorithm, it will choose and report the final color sequence. Voting algorithm is designed to report the final sequence when the following conditions is satisfied: when the same sequence is recognized more than four times consecutively, or when the number of votes exceeds the threshold value.

D.   Underwater Shape Identification

In underwater shape identification mission, ASV must detect reference buoy and build searching path, find and identify underwater shape located on designated quadrant. Technical characteristics of our approach can be divided into two parts, one is motion planning part and another is vision based perception part.

Once reference buoy can be mapped by using LIDAR sensor, In order to search the underwater shape, ASV build a lawnmower trajectory without changing its heading.[5] This is possible because out ASV is equipped with side thrusters that can generate pure sway motion.(Fig 13) By making heading angle constant during tracking the lawnmower trajectory, position error of ASV for tracking the searching parh can be minimized. In addition, since our underwater camera is mounted on starboard side of the ship, if searching path with constant margin is tracked, there will be uncovered region which may reduce detection probability of the underwater shape as in Fig 13 (right)

a) without changing heading angle   b) with changing heading angle
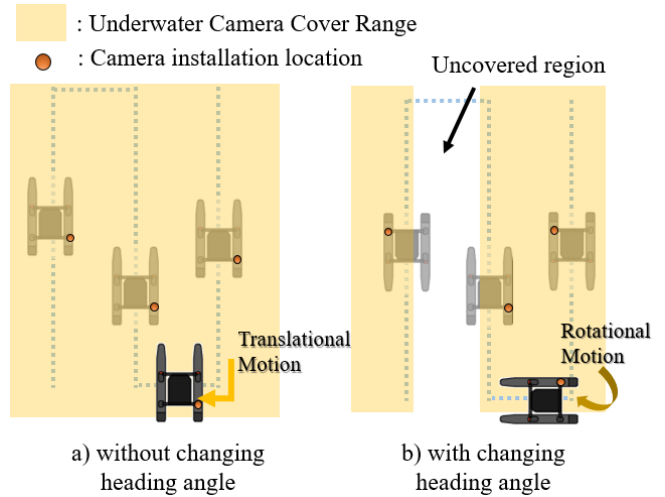
Fig. 12.Lawnmower trajectory for finding underwater shape

ASV tracks the lawnmower trajectory until underwater camera finds any object on water floor. Once any object is detected, ASV then tracks 'precise search path' instead of the lawnmower trajectory which covers whole quadrant. Precise search path is designed to cover only small area, where there is high probability of the shape to be found.

a) ASV tracking lawnmower trajectory   b) ASV tracking precise search path
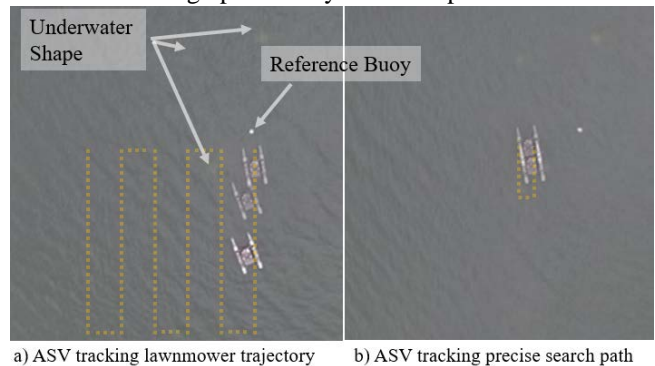
Fig. 13. Two different path tracking mode designed for underwater shape identification task

While ASV is tracking the precise search path, it decreases its surge speed drastically, so that vision system will not miss the underwater shape until it makes any identification related decision.

As ASV is tracking planned path, vision algorithm is performs perception – related decision making. While ASV is tracking lawnmower trajectory, vision system should decide whether any object is on the underwater image or not. (object detection) Once any object is detected, the motion planning part changes target path to precise search path, and vision system starts to perform identification process to the image. (object identification)

In object detection stage, we decided to use variance value of grayscale intensity of the underwater image. One of the characteristics of underwater image is its homogeniouty due to turbidity of the water. Because of this, intensity of the underwater image pixel tends to have similar value, unless

there exist some artificial structure such as the underwater shape. Variance of the image can be calculated from simple equation below. Where *I(u,v)* refers intensity value at *u,v* image coordinate and *I.mean* refers mean intensity value of the image. If the variance value exceend certain threshold, ASV consider there exist some object under water.

$$Var = \frac{1}{n} \sum_{u=1}^{u.res} \sum_{v=1}^{v.res} (I(u,v) - I.mean)^2 \qquad (4)$$
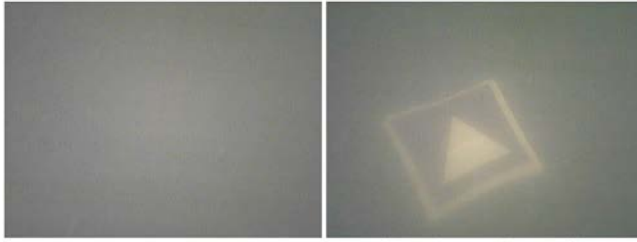
a) underwater image without
any object (variance = 353.2)

b) underwater image with
artificial object (variance = 40397.1)

Fig. 14. Underwater image and corresponding variance of intensity value

In object identification stage, vision system binarize underwater image and apply template matching algorithm to the biniary image. when making binary image, due to water turbidity, manual constant thresholding approach tends to be not suitable for underwater image binarization process. (Fig 15 b)) Instead of that, we adopted Niblack binaryzation [6] method to build binary image, which can adaptively calculate threshold to its local mask. Once the binary image matches well to shape templates, ASV reports corresponding shape as the underwater shape.

Fig. 15. Binarization of an underwater image a) original image b) Constant thresholding c) Niblack binarization method

E. Find the Break

In the Find the Break task, the ASV must extract breaks and walls from the underwater image accurately, track them based on visual data, and count the number of walls between two breaks. In order to complete the task, the ASV performs the task in four steps. At first, the ASV locates the two reference positions which can be identified by marker, buoy, or GPS position.When the reference positions are defined, the ASV moves to the first reference position and searches the break or wall from the underwater image through tracking lawnmower trajectory with fixed heading angle. If the break or wall is found, the ASV moves so that the founded object could be in the center of the image. When the object locates at the center of image, the ASV tracks breaks and walls by visual servoing counting the number of walls.

According to the task description, reference position can

be identified by marker or buoy. In this case, the ASV autonomously locates the reference position by using Lidar mapping data. The combination of two objects in clustered Lidar data that has the best match with the predefined characteristics is selected as a reference position.

The vision algorithms are applied to extract, count , and track the walls and breaks from the underwater image. Underwater image has a lot of noise due to the water turbidity and bubbles suddenly occurred. In order to detect underwater walls and breaks which are brighter than background, the V value of HSV color space is used to detect walls and breaks. The wall or break candidates are extracted through image processing such as erode or dilate filter and the candidates with a rectangular feature are filtered out as walls or breaks. Then, each wall or break is tracked using Kalman filter. [7] Fig 16 shows walls and breaks extraction result when two orange walls and one yellow break are caught on underwater image.
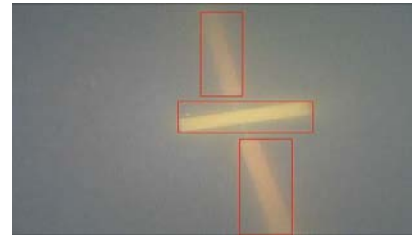
Fig. 16.Walls and breaks extraction results from underwater image

Once the wall or break is detected, the ASV moves to the position of detected object to place the object at the center of the image. The position of object can be calculated using camera calibration and depth of object information. When the detected object is at the center of image, the ASV tracks the line composed of several walls and counts the numbr of walls.
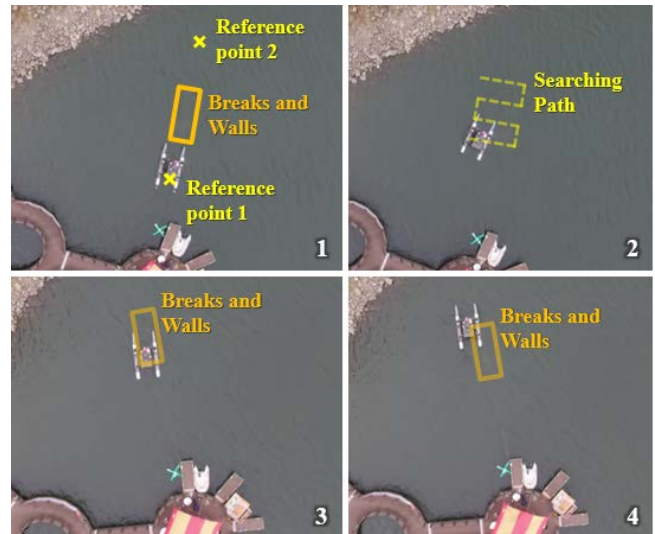
Fig. 17. Find the Break task experimental results in Jangseong-lake

Fig 17 shows top views of the ASV carrying out the Find the Break task in Jangseong-lake. First figure shows the top view of task area. The breaks and walls are installed between

two reference points. Searching path is illustrated in second figure. The ASV follows the desired searching path to detect wall or break. The path is created considering the area covered by underwater camera. The ASV keeps the position at the position of first detected wall or break, which is represented in third figure. The ASV tracks the straight line of wall segments as fourth figure.

F. Detect and Deliver

In the *detect and deliver* task, Once floating tower is detected by LIDAR mapping module, ASV approaches to floating tower and starts POI motion to find target shape or color. During the POI motion, ASV sets camera image ROI using LIDAR detection of the tower. If designated target shape or color exists in the ROI image, the search stage is finished. After that, ASV stop performing POI maneuver, instead, it performed dynamic positioning(DP) maneuver to certain point in order to maximize observability of the target hole. Calculation of the desired point can be done by using LIDAR distance sensoring. Once 2D point array can be measured from LIDAR, firstly it extract target face from the point array by using RANSAC algorithm. After that, ASV calculate the center point of the face and by calculating perpendicular artificial point infront of the face, once DP point is calculated, DP maneuver can be operated.

If DP maneuver is successfully performed, ASV starts to aim the gunbarrel toward the target hole. This can be done by using visual servoing technique. A analog camera is mounted on the Racquetball lauch module, and we have set an aiming point to image coordinate. If target hole is detected by using image processing technique, and if the hole's coordinate is coincide with the aiming point, then the Racquetball will eventually hit the target. By performing a number of experiments, we have empirically acquired a aiming point for designated relative position DP point. To move target point to the aiming point, pan and tilt motor is used to rotate Racquetball launch system. When aimed correctly, ASV command the launcher shoot the ball. After shooting, compressing and reloading procedure follows for the next ball.
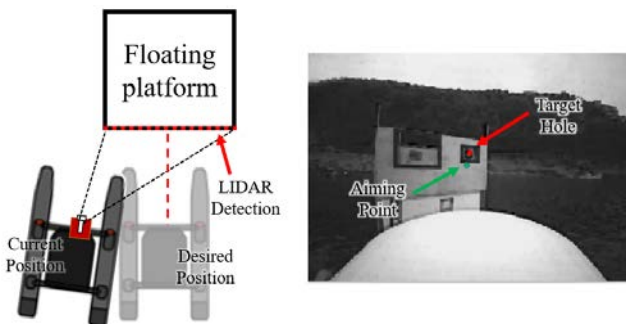
Fig. 18. Comceptual picture of LIDAR based DP (left)

To estimate the target hole center's coordinates in image plane, following image processing technique is used. The black border around two holes helps to detect the hole's edge. Canny edge detection algorithm is used to detect edge.

Among those edges, it is important to know which is the part of holes. So finding closed lines and filling the line segments is conducted. Then the candidates of the holes are obtained shown in Fig 19. Two holes's dimension in image can be measured through a number of experiments. Filtering bounding boxes based on those dimension, target hole's center coordinates are obtained shown in Fig 19.

(a) Original image   (b) Edge detection process

(c) Fill hole process   (d) Geometry constraint
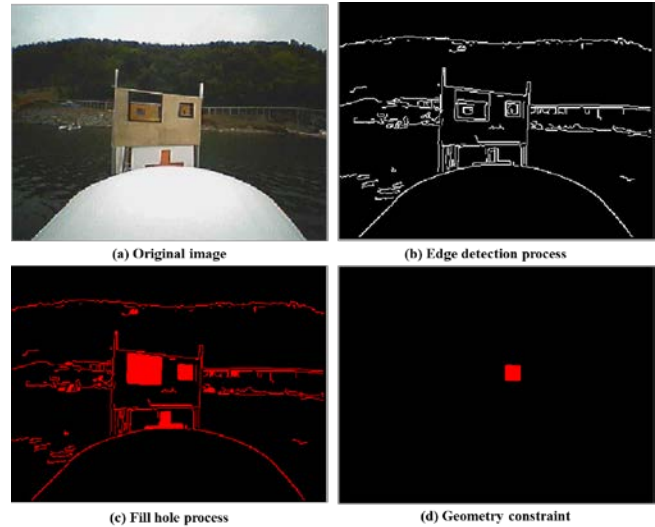
Fig. 19. Image processing procedure to estimate the target hole center's coordinate

G. Acoustic Pinger based Transit

In this task, ASV chooses an entry/exit gate where Active Pinger (AP) exists and enters via the gate → performs other tasks (or circles around a buoy which is beyond four buoys in practice/qualifying course) → returns to the starting point via the gate.

Acoustic pinger based transit task can be devided into two parts. First one is DoA θ measurement and another part is an entry/exit gate choosing part. In order to measure DOA, It requires TDoA (Time Delay of Arrival) based on onset localization of two channels from the preprocessor. Then, it chooses a gate with the maximum posterori probability of AP existence.

First, the followings describe a scheme for DoA measurement. Fig 20 illustrates a geometry for estimation of TDoA τ . $c \approx 1500\,m/s$ denotes velocity of acoustic signal in the water. A ping starting from the pinger can be detectable at ch 0 τ second prior to ping detection at ch 1 . [8]
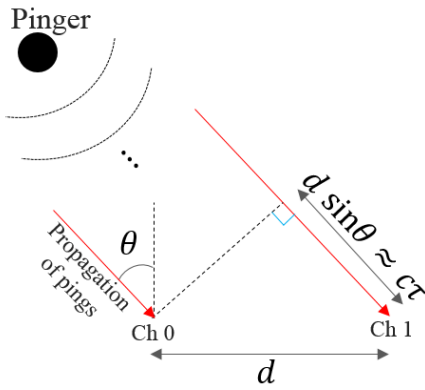
Fig. 20. A geometry for estimation of τ.

- **Step 1**: Let $x_0[k]$ be a N-point sequence sampled at ch 0 over the preprocessor during time longer than ping duration. Let f_s be sampling frequency satisfying $f_s > 4f_p$, where f_p denotes frequency of the pings.

- **Step 2**: Let $X_0[k]$, $k = 1, 2, \cdots, N$ be a DFT of $x_0[k]$. Let $X_0[k] = X_0[k]$ for $(f_p - \Delta f)N/f_s < k < (f_p + \Delta f)N/f_s$ and $(2f_p - \Delta f)N/f_s < k < (2f_p + \Delta f)N/f_s$, otherwise $X_0[k] = 0$. Let $f_0[k]$ be IFT (Inverse Fourier Transform) of the sequence.

- **Step 3**: Rescale $f_0[k]$ about the maximum value so that $|f_0[k]| \leq 1$. Let $h_0[k]$ be the rescaled $f_0[k]$. Find the first k satisfying $h_0[k] > \alpha$, where α is a threshold value. If $k < 0.05/(1/f_s)$, then set $k = k + 0.1/(1/f_s)$ and repeat the finding again. Set the returned k as k_O. Let $k_L = k_O - (r/2 - 1)$ and $k_H = k_O + (r/2 - 1)$ be RoI (Region of Interest) indices, where r is RoI size.

- **Step 4**: $h_1[k]$ can be obtained by applying **Step 2** and **Step 3** for $X_1[k]$, $k = k_L, \cdots, k_H$. Now, the scheme consider $h_0[k]$ and $h_1[k]$ for k in an interval $[k_L, k_{L,}]$.

- **Step 5**: L-point hanning window can be written as $\omega[n] = (1 - \cos(2\pi n/L))/2$, $n = 0, 1, \cdots, L-1$. Let H_0 denotes $H_0[i] = |h_0| * \omega$, $i = 0, 1, \cdots, r - L$, which is convolution of $|h_0|$ and ω. Likewise, $H_1[i] = |h_1| * \omega$. Rescaling of $H_0[i]$ and $H_1[i]$ about its maximum value makes $0 \leq H_0[i] \leq 1$ and $0 \leq H_1[i] \leq 1$, respectively.

- **Step 6**: i_0 the first onset in rescaled $H_0[i]$ can be localized by finding the first i satisfying $H_0[i] > \beta$. Using the same method, i_1 can be obtained. And τ can be obtained by $(i_1 - i_0)/f_s$, where τ denotes TDoA. From the geometry shown in Fig 20, θ is obtained as $\sin^{-1}(c\tau/d)$, where d indicates inter-distance between the hydrophones. [8]

Second, the scheme choose an entry/exit gate α_i with maximum posteriori probability, where α_i, $i = 1, 2, 3$ denotes a state of nature for entry/exit gate contains an AP in the middle of the two neighboring buoys.

A priori probability $P(\alpha_i)$ can be assumed as $P(\alpha_1) = P(\alpha_2) = P(\alpha_3)$. Then posteriori probability $P(\alpha_i | x)$ entirely depends on a conditional probability $P(x | \alpha_i)$, where x is a feature vector input on a line formed by least regression of the four buoys' positions. [9]

Distribution of $P(x | \alpha_i)$ can be modeled with the continuous normal density. When θ is given, x can be set as intersection of the line and a line starts from X_i with angle θ, where X_i is a ASV's position while performing **Step 1**.

The scheme estimates θ at a position and calculates $P(x | \alpha_i)$, $i = 1, 2, 3$. After that, the scheme repeats the above again at a different position. Let S_i be $P_0(x | \alpha_i)P_1(x | \alpha_i)$, where the subscript of P denotes a position. Finally, α_i with the maximum S_i is chosen as entry/exit gate.

Here are the experiment steps: Mapping $\rightarrow$ go to $X_0 \rightarrow$ DP (Dynamic Positioning) $\rightarrow$ TT (Turn off the Thrusters) $\rightarrow$ measure $\theta \rightarrow$ go to $X_1 \rightarrow$ DP $\rightarrow$ TT $\rightarrow$ measure $\theta \rightarrow$ choose entry/exit gate $\rightarrow$ circle around the buoy $\rightarrow$ returns to the starting point via the chosen gate.

Fig 21 shows snapshots of the task course while performing **Step 1**. $*$ indicates location of an AP.

Fig. 21. Snapshots of the task course

Measured θ at X_0 and X_1 is $-47°$ $(-49°)$ and $-15°$ $(-22°)$, respectively. The values in the parentheses are measured θ with LIDAR mapping. By the scheme, α_3 is chosen as an entry/exit gate. Now, the WAM-V enters the gate, circles around the buoy beyond the four buoys and returns to the starting point.

IV. CONCLUSION

SNU Marco have developed an innovative ASV system. This includes specially designed motion mode and propulsion system, objects or symbols detection and identification algorithm, underwater aucoustic signal anlysis system and pneumatic ball launcher system. These innovations are expected to contribute to the development of

autonomous robotic systems in the marine domain as well as 2016 Maritime RobotX Challenge.

REFERENCE

[1] Manley, Justin E. (2008, Sep) Unmanned surface vehicles, 15 years of development. MTS/IEEE OCEANS 2008 Conference. [Online]. Available: http://ieeexplore.ieee.org/document/5152052/

[2] Park, Jeonghong, et al. (2016, JUNE) Development of an Unmanned Surface Vehicle System for the 2014 Maritime RobotX Challenge. Journal of Field Robotics. [Online]. Available: http://onlinelibrary.wiley.com/doi/10.1002/rob.21659/abstract

[3] Campbell S, Abu-Tair M and Naeem W, "An automatic COLREGs-compliant obstacle avoidance system for an unmanned surface vehicle," Proceedings of the Institution of Mechanical Engineers, Part M: Journal of Engineering, 2013, pp. 566-578.

[4] K.S. Fu, et al., "Robotics: Control, Sensing, Vision, and Intelligence," McGraw-Hill Book Company, 1987.

[5] Pyo, Juhyun, et al. (2015, Nov) Development of hovering type AUV "Cyclops" and its performance evaluation using image mosaicking. Ocean Engineering 109. [Online] pp. 517-530. Available: http://www.sciencedirect.com/science/article/pii/S0029801815004953

[6] W. Niblack, "An introduction to digital image processing," Strandberg Publishing Company, 1985.

[7] Beymer, D., and Konolige, K., "Real-time tracking of multiple people using continuous detection," IEEE International Conference on Computer Vision(ICCV) Frame-Rate Workshop, 1999.

[8] J. Benesty, J. Chen and Y. Huang. "Microphone array signal processing (Vol. 1)," Springer Science & Business Media, 2008

[9] J. P. Bello, L. Daudet, S. Abdallah, C. Duxbury, M. Davies and M. B. Sandler, M. B. A tutorial on onset detection in music signals. IEEE Trans. Speech Audio Process, Vol. 13, No. 5, pp. 1035-1047, Sep, 2005.

[10] R. O. Duda, P. E. Hart and David G. Stork, "Pattern classification," John Wiley & Sons, 2012.